DOI: 10.1002/asia.200800227

Elaboration of *rac*-Like Active Species from Lewis Base Functionalized Unbridged Zirconocenes for Isospecific Propylene Polymerization

Hwa Kyu Kim, Seong Kyun Kim, Jun Ha Park, Seung Woong Yoon, Min Hyung Lee,* and Youngkyu Do*[a]

Abstract: A series of *ortho* or *meta* Lewis base functionalized unbridged zirconocenes, [{1-(E$_n$-Ph)-3,4-Me$_2$C$_5$H$_2$}$_2$ZrCl$_2$] (E = NMe$_2$, OMe; n = 1, 2), and a half-functionalized zirconocene, [{1-(*p*-Me$_2$NC$_6$H$_4$)-3,4-Me$_2$C$_5$H$_2$}{1-(*p*-tolyl)-3,4-Me$_2$C$_5$H$_2$}ZrCl$_2$], were prepared. The crystal structures of these compounds determined by X-ray diffraction revealed the presence of only C_2-symmetric *rac*-like isomers in the asymmetric units. In combination with methylaluminoxane (MAO) cocatalyst, the *meta*-functionalized complexes afforded mixtures of polymers that exhibit multimelting transition temperatures and broad molecular-weight distributions (MWDs) in propylene polymerization at atmospheric monomer pressure, whereas the *ortho*-functionalized complexes did not give rise to polymerization. Stepwise solvent extraction of the polymer mixtures showed that the polymers consist of amorphous, moderately isotactic, and highly isotactic portions, the weight ratio of which is dependent on the reaction temperature. ^{13}C NMR spectral analysis indicated that the [*mmmm*] methyl pentad value of the isotactic portion reached around 90%. Among the *meta*-functionalized zirconocenes, the di-OMe-substituted one afforded the largest amount of the isotactic portion at all temperatures, and the portion comprised 82 wt% of the crude polymer obtained at 25 °C. In contrast, propylene polymerization with the half-functionalized unbridged zirconocene resulted in the formation of nearly atactic polypropylene with a narrow MWD of around 2. These results corroborate the proposition that the rigid *rac*-like cation–anion ion pair of type [*rac*-L$_2$ZrP]$^+$[Me-MAO]$^-$ generated in situ, through Lewis acid–base interactions between the functional groups and [Me-MAO]$^-$, is responsible for the isospecific propylene polymerization with the given class of functionalized unbridged zirconocenes and further indicate that the formation of such ion pairs can be favored by difunctionalization at the *meta* position of the phenyl ring with OMe groups.

Keywords: Lewis bases · metallocenes · polymerization · polymers · zirconium

Introduction

The correlation between the nature of single-site catalytic systems based on Group 4 metal complexes and the properties of the resulting polymers has been well-established over the last few decades.[1–10] In particular, the structure–property relationship between the coordination geometry of the catalyst precursors and the stereoregularity of polypropylene in propylene polymerization has attracted great attention owing to the various opportunities to tailor the microstructure and thereby the physical properties of polypropylenes.[11] Through proper manipulation of the catalyst structure, highly isotactic and syndiotactic polypropylenes can now be easily accessible from *ansa*-metallocene catalysts with a fixed geometry of C_2 and C_s symmetries, respectively.[9–16]

Less focus, however, has been placed on unbridged metallocenes owing to their aspecific nature in propylene polymerization. Nonetheless, several unbridged metallocene catalyst systems that exhibit stereospecific polymerization of propylene have been achieved through variation of the cyclopentadienyl ligand. For example, Erker et al. showed that catalysts with a bulky ligand can induce isospecific polymerization at a relatively low polymerization temperature (**I**; Scheme 1),[17–20] and Waymouth and co-workers demonstrated that geometry switching between *rac*-like and *meso*-like isomers of [(2-PhInd)$_2$ZrCl$_2$] systems (**II**; Scheme 1) leads to the formation of isotactic–atactic stereoblock polypropy-

[a] H. K. Kim, Dr. S. K. Kim, J. H. Park, S. W. Yoon, Dr. M. H. Lee, Prof. Dr. Y. Do
Department of Chemistry
School of Molecular Science-BK21
KAIST, Daejeon 305-701 (Korea)
Fax: (+82) 42-350-2810
E-mail: lmh74@kaist.ac.kr
ykdo@kaist.ac.kr

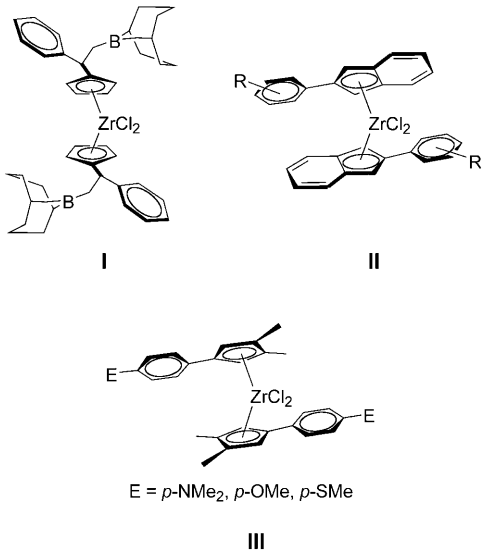

Scheme 1.

lene,[21–30] which was recently re-interpreted by Busico et al. that cation–anion "interlocking" is responsible for the stereocontrol.[31,32] Razavi and Atwood also reported that bis(1-methylfluorenyl)zirconium dichloride can produce isotactic polypropylene with an [*mmmm*] methyl pentad content of 83% at temperatures of around 60°C.[33] All these findings are based on the introduction of hindered ligand rotation in the catalyst structure during the course of isospecific propylene insertion.

When the industrial significance of the production of isotactic polypropylene and the merit of synthetically easy accessibility are considered, it is still of great interest to develop unbridged metallocene catalytic systems capable of inducing isospecific polymerization of propylene. In this regard, our group recently disclosed a novel synthetic strategy for the synthesis of isotactic polypropylene by using various *para*-Lewis base substituted unbridged zirconocenes in combination with methylaluminoxane (MAO) cocatalyst (**III**; Scheme 1).[34,35] It was revealed that the interaction of Lewis acidic sites in [Me-MAO]$^-$ with Lewis basic atoms of functionalized unbridged zirconocene cations prevents rapid ligand rotation, thus leading to the formation in situ of rigid C_2-symmetric-like cation–anion ion pairs for isospecific polymerization. We also found that the amount of the isotactic portion of the resulting polypropylene is affected by the strength of the Lewis acid–base interactions.[35] Although the foregoing findings indicate that such Lewis acid–base interaction is primarily responsible for the isospecific propagation of propylene, it would be intriguing to investigate the optimum functionalization on the phenyl ring in terms of the position and the number of functional groups to achieve higher isospecificity, as well as to maximize the amount of the isotactic portion, from which detailed aspects of the stereocontrol occurring in the given class of unbridged metallocene systems would be understood.

To this end, we prepared new derivatives of general formula [1-(E_n-Ph)-3,4-$Me_2C_5H_2$]$_2ZrCl_2$ (E = NMe_2, OMe; n = 1, 2), in which the Lewis basic group E was singly or doubly introduced at the *ortho* or *meta* position of the phenyl ring, and their propylene-polymerization behavior was examined. Finally, to elucidate experimentally our proposition that rigid *rac*-like cationic active species generated in situ are responsible for the isospecificity, the propylene-polymerization properties of a half-functionalized unbridged zirconocene were also investigated.

Results and Discussion

Synthesis and Characterization

Synthetic routes to the *ortho* and *meta* Lewis base functionalized ligands and the corresponding zirconocenes are depicted in Scheme 2. Reaction of Grignard reagents (for ***o*O1** and ***m*O1**) or lithium salts (for ***m*O2**, ***o*N1**, ***m*N1**, and ***m*N2**) of E_n-substituted bromobenzene (E = *o*- or *m*-NMe_2 and OMe; n = 1, 2) with 1 equivalent of 3,4-dimethylcyclopent-2-enone in THF followed by dehydration with *p*-TsOH or HCl afforded the desired final ligands, 1-(E_n-Ph)-3,4-$Me_2C_5H_3$. For the preparation of the ***m*N2** ligand, 1-Br-3,5-$(Me_2N)_2C_6H_3$ was newly synthesized according to a modification of the literature procedure[36] and employed as starting material.

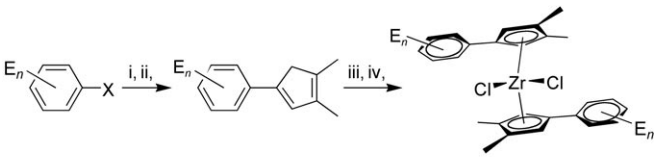

	E_n	X
***o*N1**	2-NMe_2	Li
***m*N1**	3-NMe_2	Li
***m*N2**	3,5-$(NMe_2)_2$	Li
***o*O1**	2-OMe	MgBr
***m*O1**	3-OMe	MgBr
***m*O2**	3,5-$(OMe)_2$	Li

	E_n
***o*ZrN1**	2-NMe_2
***m*ZrN1**	3-NMe_2
***m*ZrN2**	3,5-$(NMe_2)_2$
***o*ZrO1**	2-OMe
***m*ZrO1**	3-OMe
***m*ZrO2**	3,5-$(OMe)_2$

Scheme 2. Synthesis of *ortho* and *meta* Lewis base functionalized unbridged zirconocenes. Reaction conditions: i) 3,4-Dimethylcyclopent-2-enone/THF; ii) *p*-TsOH/CH_2Cl_2 or aq. HCl; iii) *n*BuLi/Et_2O; iv) $^1/_2$ [$ZrCl_4(thf)_2$]/toluene.

The synthesis of unbridged zirconocenes was achieved by the transmetalation of lithium salts of the ligands with 0.5 equivalent of [$ZrCl_4(thf)_2$] in toluene. All the zirconocenes were obtained as light-yellow solids in moderate yields (40–50%). Any interference in the transmetalation caused by the *ortho* or *meta* Lewis base functionalities was not observed. To prepare a half-functionalized unbridged zirconocene, on the other hand, we chose the zirconocene [{1-(*p*-$Me_2NC_6H_4$)-3,4-$Me_2C_5H_2$}{1-(*p*-tolyl)-3,4-$Me_2C_5H_2$}$ZrCl_2$] (**ASZr**), which bears mixed Cp (cyclopentadienyl) ligands in which the NMe_2 and Me groups are at-

tached on the *para* position of each phenyl ring. The synthesis of **ASZr** includes the initial preparation of [{1-(*p*-tolyl)-3,4-$Me_2C_5H_2$}$ZrCl_3$][37,38] followed by treatment of it with Li[1-(*p*-$Me_2NC_6H_4$)-3,4-$Me_2C_5H_2$][28,39] (Scheme 3).

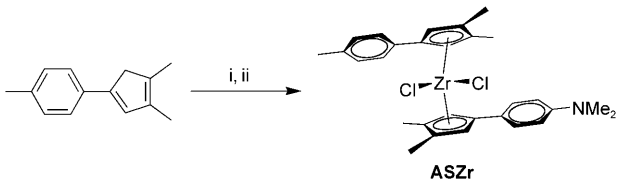

Scheme 3. Synthesis of a half-functionalized unbridged zirconocene. Reaction conditions: i) *n*BuLi/Et_2O, Me_3SiCl/THF, $ZrCl_4$/*n*-heptane; ii) Li[1-(*p*-$Me_2NC_6H_4$)-3,4-$Me_2C_5H_2$]/toluene.

The solid-state structures of selected complexes ***o*ZrN1**, ***m*ZrN1**, ***o*ZrO1**, ***m*ZrO2**, and **ASZr** were determined by X-ray diffraction studies. Single crystals suitable for X-ray structural determination were obtained by cooling solutions of CH_2Cl_2/*n*-hexane or diethyl ether/*n*-hexane to −20 °C. The molecular structures are shown in Figure 1, and Tables 1 and 2 summarize the detailed crystallographic data and selected interatomic distances and angles, respectively. The ***o*ZrN1**, ***m*ZrN1**, and ***m*ZrO2** complexes crystallize in the space group $P\bar{1}$, whereas ***o*ZrO1** and **ASZr** crystallize in the space groups $P2_1/c$ and $P2_1/n$, respectively. Interestingly, only the C_2-symmetric *rac*-like isomers were seen in the asymmetric units of all the structures, as similarly observed in the *para*-functionalized unbridged zirconocenes reported previously.[34,35] Whereas the Zr−Cl and Zr−Cg (ring centroid) bond lengths/distances and the Cl1-Zr-Cl2 and Cg1-Zr-Cg2 angles are nearly similar to those of the related unbridged zirconocenes,[28,40,41] including the *para*-functionalized zirconocenes, the *meta*-functionalized dimethoxy complex ***m*ZrO2** showed the smallest Cl1-Zr-Cl2 and the largest Cg1-Zr-Cg2 angle among the series of functionalized zirconocenes. Notably, the dihedral angle between the Cp and phenyl rings is affected by the position and the number of the functional group: 1) the angle decreases in the order *ortho*-, *meta*-, and *para*-functionalized zirconocenes with monosubstitution (***o*ZrN1** and ***o*ZrO1** vs. ***m*ZrN1** vs. **ASZr**); 2) the NMe_2-functionalized zirconocene forms a larger angle than the OMe-functionalized one (***o*ZrN1** vs. ***o*ZrO1**); and 3) the greater the substitution, the larger the resulting angle (***m*ZrO2** vs. ***m*ZrN1**). These features are consistent with the steric effect between the Cp and phenyl rings, which may interfere with the electronic conjugation capable of leading to planar geometry in the ligand fragment.

Propylene Polymerization

Bis-Type Functionalized Zirconocenes

Propylene polymerization with all the zirconocenes ***o*ZrN1**, ***o*ZrO1**, ***m*ZrN1**, ***m*ZrO1**, ***m*ZrN2**, ***m*ZrO2**, and **ASZr** were carried out at various temperatures under MAO activation at atmospheric monomer pressure. The *meta*-functionalized zirconocenes produced polypropylenes with moderate to low activities, whereas the *ortho* analogues did not result in any polymerization under the given conditions, probably owing to the large steric hindrance of the *ortho* substituents (Table 3). The activities of the *meta*-functionalized zirconocenes were lower than those of the corresponding *para*-functionalized ones [{1-(E-Ph)-3,4-$Me_2C_5H_2$}$_2ZrCl_2$] (E = *p*-NMe_2 (***p*ZrN1**), *p*-OMe (***p*ZrO1**)),[34,35] which indicates that propylene-insertion reactions are retarded by steric effect from the *meta* substituents on the phenyl ring. Among the *meta*-functionalized zirconocenes, the OMe-substituted zirconocenes were more active than the NMe_2-substituted ones at all temperatures. Consistent with these results is the observation that the difunctionalized ***m*ZrN2** produced negligible amounts of polypropylene under the given conditions, whereas ***m*ZrO2** exhibited moderate activity comparable to that of the monosubstituted ***m*ZrO1**.

The crude polypropylenes obtained with the *meta*-functionalized zirconocenes ***m*ZrN1**, ***m*ZrO1**, and ***m*ZrO2** displayed broad molecular-weight distributions (MWD, M_w/M_n) ranging from 3.7 to 14.1, which indicates the involvement of multicatalytic

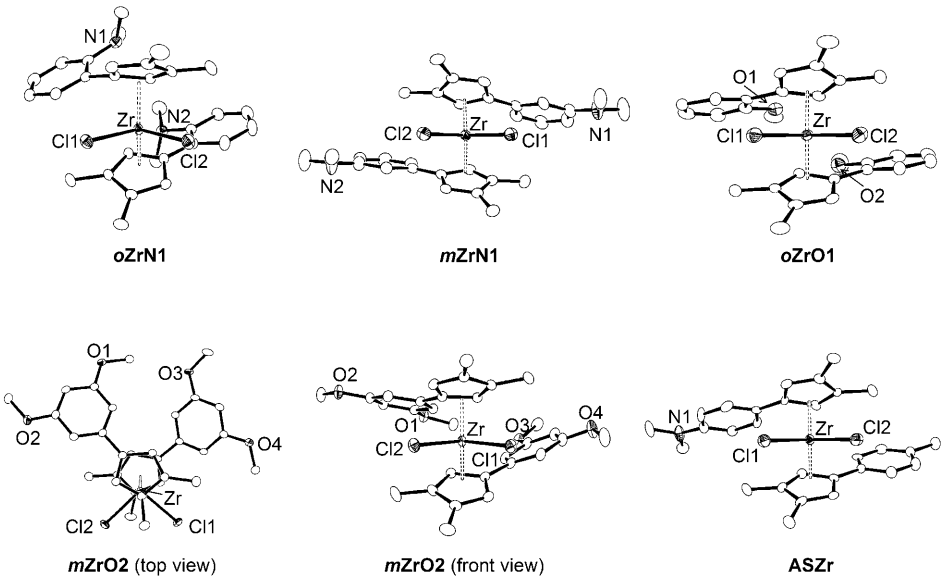

Figure 1. Crystal structures of ***o*ZrN1**, ***m*ZrN1**, ***o*ZrO1**, ***m*ZrO2**, and **ASZr** (35% ellipsoid probability). H atoms and solvent molecules are omitted for clarity.

Table 1. Crystallographic data and parameters for ***o*ZrN1**, ***m*ZrN1**, ***o*ZrO1**, ***m*ZrO2**, and **ASZr**.

Compounds	***o*ZrN1**	***m*ZrN1**	***o*ZrO1**	***m*ZrO2**	**ASZr**
Formula	$C_{30}H_{36}Cl_2N_2Zr$	$(C_{30}H_{36}Cl_2N_2Zr)_2$	$C_{28}H_{30}Cl_2O_2Zr$	$C_{30}H_{34}Cl_2O_4Zr$	$C_{29}H_{33}Cl_2NZr$
Formula weight	586.73	1173.46	560.64	620.69	557.68
Crystal system	triclinic	triclinic	monoclinic	triclinic	monoclinic
Space group	$P\bar{1}$	$P\bar{1}$	$P2_1/c$	$P\bar{1}$	$P2_1/n$
a [Å]	9.3442(19)	12.9660(7)	11.2537(4)	9.1088(18)	13.5258(13)
b [Å]	10.547(2)	15.3702(9)	13.7928(5)	12.204(2)	14.0667(17)
c [Å]	15.361(3)	16.0674(8)	20.4420(8)	13.872(3)	14.1561(16)
α [°]	78.33(3)	62.796(2)	90.00	95.43(3)	90.00
β [°]	77.58(3)	85.956(2)	95.451(2)	102.21(3)	105.055(8)
γ [°]	71.93(3)	87.752(2)	90.00	108.12(3)	90.00
V [Å^3]	1390.5(5)	2840.7(3)	3158.7(2)	1411.0(5)	2600.9(5)
Z	2	2	4	2	4
ρ_{calcd} [g cm^{-3}]	1.401	1.372	1.179	1.461	1.424
μ [mm^{-1}]	0.609	0.596	0.536	0.613	0.646
$F(000)$	608	1216	1152	640	1152
T [K]	130(2)	130(2)	130(2)	130(2)	130(2)
θ range [°]	2.05–34.89	1.43–35.45	1.82–30.81	1.52–31.50	1.86–20.87
hkl range	−15→14, −16→16, −24→20	−21→15, −25→25, −25→26	−16→16, −14→19, −29→27	−13→13, −16→17, −20→20	−13→13, −14→14, −14→14
Measured reflns	33833	39651	41795	37739	16470
Unique reflns (R_{int})	10978 (0.0566)	22966 (0.0480)	9801 (0.0762)	8883 (0.0513)	2732 (0.1626)
Reflns used for refinement	10978	22966	9801	8883	2732
Refined parameters	324	648	378	342	305
$R1$[a] ($I>2\sigma(I)$)	0.0420	0.0447	0.0530	0.0349	0.0421
$wR2$[b] (all data)	0.1194	0.1218	0.1366	0.1136	0.1266
GOF on F^2	1.005	1.006	1.025	1.009	1.056
ρ_{fin} (max/min) [e Å^{-3}]	0.980, −1.365	0.787, −0.552	0.527, −0.712	0.549, −0.947	0.386, −0.391

[a] $R1=\Sigma||F_o|-|F_c||/\Sigma|F_o|$. [b] $wR2=\{[\Sigma w(F_o^2-F_c^2)^2]/[\Sigma w(F_o^2)^2]\}^{1/2}$.

Table 2. Selected bond lengths/distances [Å] and angles [°] for ***o*ZrN1**, ***m*ZrN1**, ***o*ZrO1**, ***m*ZrO2**, and **ASZr**.

Compounds	***o*ZrN1**	***m*ZrN1**	***o*ZrO1**	***m*ZrO2**	**ASZr**
Zr–Cl1	2.4437(10)	2.4528(6)	2.4498(8)	2.4459(8)	2.456(2)
Zr–Cl2	2.4377(10)	2.4478(6)	2.4439(8)	2.4436(9)	2.446(2)
Zr–Cg1[a]	2.2227(11)	2.2225(10)	2.2116(12)	2.2257(11)	2.218(4)[b]
Zr–Cg2[a]	2.2227(10)	2.2219(10)	2.2130(14)	2.2194(12)	2.230(4)
Cl1-Zr-Cl2	96.12(3)	96.90(2)	95.65(3)	95.51(3)	96.43(9)
Cg1-Zr-Cg2	131.87(5)	131.24(4)	129.96(5)	132.75(5)	130.19(14)
Cp1-Ph1[c]	45.09(13)	12.71(13)	20.95(16)	13.82(12)	5.1(4)
Cp2-Ph2[c]	21.94(13)	19.01(13)	18.1(4)	29.49(13)	7.0(4)

[a] Cg = centroid of Cp ring. [b] The Cp ring bearing a *p*-NMe_2 group. [c] Dihedral angles between the planes.

active species in the *meta*-functionalized zirconocene/MAO catalyst systems. Although the MWD values from ***m*ZrN1** were in a relatively narrow range of around 4 at all temperatures, the multimodality was clearly seen for the polymers from the OMe-functionalized ***m*ZrO1** and ***m*ZrO2** with a decreased MWD value at high temperature. For example, the GPC (gel-permeation chromatography) curves for the polymers obtained with ***m*ZrO2** are shown in Figure 2. Despite inactivity in propylene polymerization, ethylene polymerization with the difunctionalized ***m*ZrN2** was further investigated at relatively high temperature to see if the multicatalytic active species can be formed in situ. The results show that ***m*ZrN2** did produce high-molecular-weight polyethylene with a broad MWD, thus confirming the generation of the multicatalytic active species upon MAO activation (Table 3, runs 19 and 20). In agreement with the GPC results, DSC (differential scanning calorimetry) diagrams of the polymers from ***m*ZrN1**, ***m*ZrO1**, and ***m*ZrO2** exhibited multimelting transitions with a maximum T_m value ranging from 129 to 159 °C, which indicates the formation of a mixture of polypropylenes of different crystallinity. Although the T_m value gradually deceased as the reaction temperature increased, the apparent melting transition of the polypropylene produced at 70 °C reflects the formation of crystalline polypropylene even at high temperature.

The selected crude-polymer samples were further fractionated by stepwise solvent extraction into three portions: diethyl ether soluble, diethyl ether insoluble and *n*-heptane-soluble, and diethyl ether insoluble and *n*-heptane-insoluble portions. As reported earlier,[42] these portions correspond to atactic-like, moderately isotactic, and highly isotactic polypropylene, respectively. The methyl regions of the ^{13}C NMR spectra for the *n*-heptane-insoluble portions obtained with ***m*ZrN1**, ***m*ZrO1**, and ***m*ZrO2** at 25 °C exclusively show the peak attributable to the [*mmmm*] methyl pentad sequence, in conjunction with very small peaks for the stereoerrors originating from the site-controlled mechanism that matches with the ratio [*mmmr*]/[*mmrr*]/[*mrrm*] ≈ 2:2:1 (Figure 3).[12,43] Most remarkably, the calculated [*mmmm*] values reached around 90 %, which is as high as those obtained with the *para*-functionalized zirconocenes and the well-known isospecfic, C_2-symmetric catalysts.[12] This result indicates that the *meta*-functionalized zirconocenes are able to induce isospecific polymerization of propylene in combi-

Table 3. Propylene polymerization data with bis-type functionalized zirconocenes and **ASZr**.[a]

Run	Catalyst	t_p [h]	T_p [°C]	Activity [(kg PP)/((mol Zr) h bar)]	M_w[b] $\times 10^{-3}$	M_w/M_n[b]	T_m[c] [°C]	Diethyl ether soluble [wt %]	Diethyl ether insoluble/ *n*-heptane soluble [wt %]	Diethyl ether insoluble/ *n*-heptane insoluble [wt %]	[*mmmm*][d]
1	***o*ZrN1**	2	25, 50	trace							
2	***m*ZrN1**	2	0	2	201	4.05	156.2	n.d.	n.d.	n.d.	
3		2	25	35	12	3.69	150.0	28	38	34	0.90
4		2	50	29	157	4.10	139.5	42	24	18	
5		2	70	4	207	4.43	133.8	n.d.	n.d.	n.d.	
6	***m*ZrN2**	2	25, 50	trace							
7	***o*ZrO1**	2	25, 50	trace							
8	***m*ZrO1**	2	0	9	223	4.23	159.3	n.d.	n.d.	n.d.	
9		2	25	52	57	10.0	152.1	15	38	47	0.91
10		2	50	192	183	14.1	144.4	27	48	25	
11		2	70	104	195	4.15	129.3	47	53	0	
12	***m*ZrO2**	4	0	18	101	9.37	155.7	n.d.	n.d.	n.d.	
13		2	25	69	51	8.09	155.0	9	9	82	0.87
14		2	50	126	36	8.18	146.6	25	14	61	
15		2	70	117	14	4.75	134.6	26	45	29	
16	**ASZr**	2	0	1046	72	2.13	n.o.	93	7	0	
17		1	25	1846	28	2.85	n.o.	98	2	0	
18		1	50	1196	4	2.08	n.o.	100	0	0	
19[e]	***m*ZrN2**	0.5	50	170	386	12.4	135.0				
20[e]		1	70	292	304	11.5	133.4				

[a] Polymerization conditions: P(propylene) = 1 bar, [Zr] = 5.0 μmol, cocatalyst = MAO, [Al]/[Zr] = 1000, solvent = 50 mL toluene. [b] Determined by GPC. [c] Determined by DSC. [d] Determined by ^{13}C NMR spectroscopy. [e] Ethylene polymerization: P(ethylene) = 1 bar. PP = polypropylene, n.d. = not determined, n.o. = not observed.

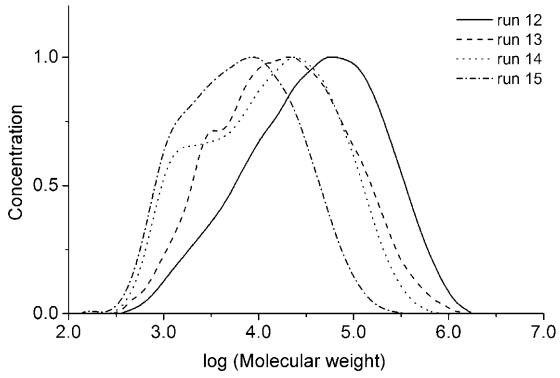

Figure 2. GPC curves for the polypropylenes obtained with ***m*ZrO2** at 0, 25, 50, and 70 °C (Table 3, runs 12–15, respectively).

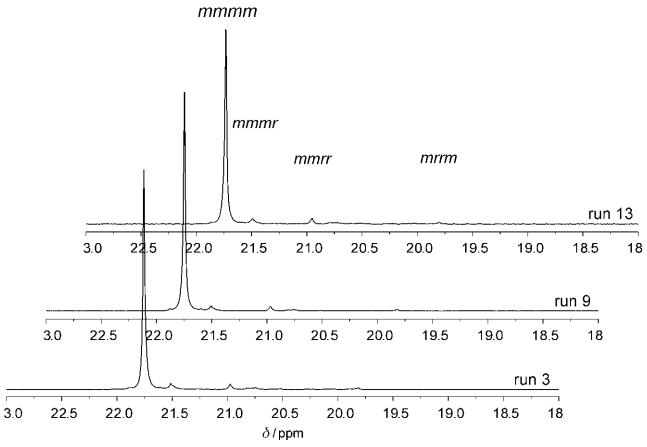

Figure 3. ^{13}C NMR spectra of the *n*-heptane-insoluble portions of the polypropylenes obtained with ***m*ZrN1**, ***m*ZrO1**, and ***m*ZrO2** at 25 °C (Table 3, runs 3, 9, and 13, respectively).

nation with MAO cocatalyst. The formation of highly isotactic polypropylene is also consistent with the observation of high T_m values of the crude polypropylene as described above.

The amount of the *n*-heptane-insoluble portion of polymer decreased with increasing reaction temperature, whereas those of the diethyl ether soluble and *n*-heptane-soluble portions increased, which indicates that the thermal equilibria between active species responsible for each extracted portion are largely affected by temperature. Among the *meta*-functionalized zirconocenes, ***m*ZrO2** afforded the largest amount of the *n*-heptane-insoluble portion at all temperatures. In particular, the *n*-heptane-insoluble portion from ***m*ZrO2** comprised 82 wt % of the crude polypropylene obtained at 25 °C, thus reflecting the prevailing isotactic propagation of propylene in the polymerization. This amount is even larger than those from the *para*-functionalized zirconocenes (***p*ZrN1** and ***p*ZrO1**) reported previously under the same reaction conditions.[34,35] ***m*ZrO2** also gave rise to an appreciable amount of the highly isotactic portion (29 wt %) at 70 °C, whereas ***m*ZrO1** gave hardly any (≈0 wt %). These results suggest that the difunctionalization by OMe groups at the *meta* position of the phenyl ring is much in favor of the formation in situ of rigid C_2-symmetric-like cation–anion ion pairs of the type [*rac*-L_2ZrP]$^+$[Me-MAO]$^-$ for isospecific propagation, and the resulting ion pair is effectively maintained during the polymerization even at elevated temperature. The increased chance of Lewis acid–base interactions

from two functional groups on the phenyl ring is probably responsible for this feature. The OMe-substituted ***m*ZrO1** produced more *n*-heptane-insoluble portion than the more Lewis basic, NMe_2-substituted ***m*ZrN1** (Table 3, runs 3 vs. 9 and 4 vs. 10), although the difference was not large. This observation is somewhat contrary to the previous result obtained with *para*-functionalized zirconocene systems, in which the amount of the isotactic portion decreased in the order of decreasing Lewis basicity of the functional group, that is, $NMe_2 > OMe > SMe$.[35] This result might be ascribed to the increased steric hindrance between the functional groups and the MAO anion possibly due to the narrower interaction space for the *meta*-functionalized zirconocenes than the *para* ones, which could thus affect the Lewis acid–base interactions required for the formation of C_2-symmetric-like ion pairs. ***m*ZrO1**, which bears a small OMe group with two O(sp^3) lone-pair electrons, appears not to be affected by steric hindrance, thus rendering it suitable for attaining such interactions, unlike ***m*ZrN1**, which probably suffers from steric hindrance due to a relatively bulky NMe_2 group. In fact, the isotactic portions obtained with ***m*ZrO1** were of quite similar amounts to those with the *para*-OMe-functionalized zirconocene (***p*ZrO1**) at various temperatures under atmospheric monomer pressure.[35] Furthermore, this steric consideration associated with the formation of *rac*-like ion pairs is in parallel with the activity trends, such as the inferior activity of ***m*ZrN1** relative to ***m*ZrO1** and the inactivity of ***m*ZrN2**, which probably result from the interference of the noninteracting, free *meta*-NMe_2 group with the insertion of propylene monomer. Another explanation for the less isotactic portion with ***m*ZrN1** might be due to the improper conformational orientation of the *meta*-NMe_2 group for achieving effective interaction with the bulky MAO anion. For effective interaction, the lone-pair electrons of the nitrogen atom should point toward a more open rear end, which may require the ligands to be slightly rotated. As a result, this could lead to structural change of the C_2-symmetric-like active species responsible for the isospecific propagation of propylene, thus producing an increase in the lower-tacticity portions.

Half-Functionalized Zirconocene (ASZr)

To elucidate experimentally our proposition that rigid *rac*-like cationic active species generated in situ are the origin for the observed high isospecificity, the propylene-polymerization behavior of a half-functionalized unbridged zirconocene, **ASZr**, was explored at various temperatures (Table 3). The **ASZr**/MAO catalytic system showed increased activity relative to the *meta*- and *para*-functionalized bis-type zirconocenes, but produced polypropylene of which molecular weight was quite low and decreased with increasing temperature (Table 3, runs 16–18). Most interestingly, the crude polypropylene exhibited a narrow MWD of around 2 with a unimodal feature, which suggests that this catalytic system consists almost entirely of a single-active-site catalyst (Figure 4). Furthermore, the stepwise solvent extraction and the ^{13}C NMR spectra reveal that the crude polypropylene

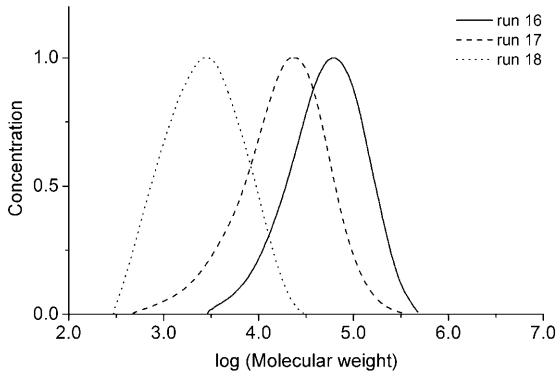

Figure 4. GPC curves for the polypropylenes obtained with **ASZr** at 0, 25, and 50 °C (Table 3, runs 16–18, respectively).

produced at 0 °C contained 93 wt % of diethyl ether soluble ([*mmmm*] ≈ 14 %) and 7 wt % of *n*-heptane-soluble ([*mmmm*] ≈ 32 %) portions, whereas the polymers obtained at 25 and 50 °C were composed almost entirely of diethyl ether soluble portions. The [*mmmm*] value of the *n*-heptane-soluble portion implies the formation of slightly isorich polypropylene from **ASZr**/MAO, which could also be indicative of the presence of Lewis acid–base interaction between the cationic active species from **ASZr** and the MAO anion, which can induce hindered ligand rotation. However, this isotacticity is still lower than that obtained with the related *para*-functionalized zirconocene ***p*ZrN1**, which afforded 53–67 % of the [*mmmm*] values for the *n*-heptane-soluble portion at various temperatures. As the *n*-heptane-soluble portion could include low-molecular-weight but highly isotactic polypropylene, DSC analysis was used for further investigation. Although the DSC diagram shows essentially no melting transition for the crude polymer, inspection of the *n*-heptane-soluble portion revealed a very broad, weak melting transition ranging from around 60 to 140 °C without any indication of distinct high-melting peaks. This result is somewhat different from the high-melting peaks at around 150 °C observed for the *n*-heptane-soluble portion from ***p*ZrN1**. Overall, it can be said that **ASZr**/MAO produces nearly atactic polypropylenes. The low-molecular-weight polymers from **ASZr** are also in good agreement with the formation of low-tacticity polypropylene, as similarly observed for *para*-SMe-functionalized zirconocene.[35]

These findings indicate that when the heteroatom is functionalized only at one side of the ligands, the resulting catalytic active species are not able to induce isospecific propagation of propylene. In other words, the Lewis acid–base interaction between one ligand of zirconocene and the MAO anion is not sufficient to prevent the ligands from rapidly rotating in solution; thus, it is hardly capable of leading to the C_2-symmetric-like active species required for isospecific propagation. Therefore, these results support our proposition that the generation in situ of rigid *rac*-like cation–anion ion pairs of the type $[rac\text{-}L_2ZrP]^+[Me\text{-}MAO]^-$ through Lewis acid–base interactions between the functional groups

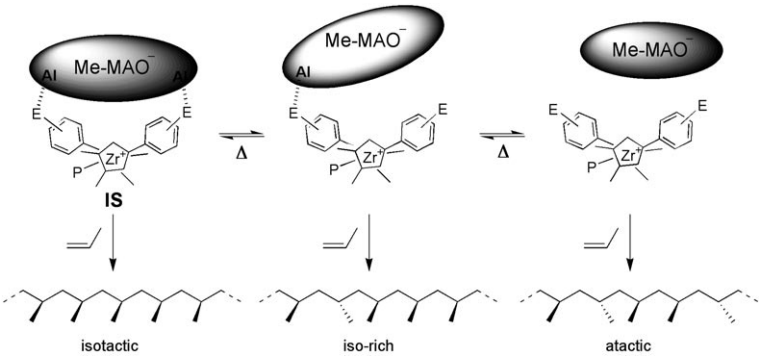

Scheme 4. Proposed thermal equilibria and the propagation of propylene with the possible active species from *para* or *meta* Lewis base (E = NMe_2, OMe) functionalized unbridged zirconocenes upon MAO activation.

and [Me-MAO]$^-$ is responsible for isospecific propylene polymerization with the given class of functionalized unbridged zirconocenes (**IS**; Scheme 4). Furthermore, it could also be suggested that each of the active species in the thermal equilibria is involved in the propagation of propylene with different stereospecificity, that is, isotactic, iso-rich, and atactic propagation, respectively (Scheme 4).

Conclusions

A series of *ortho* or *meta* Lewis base functionalized unbridged zirconocenes was prepared, and their catalytic properties toward propylene polymerization were investigated under MAO activation at atmospheric monomer pressure. Whereas the *ortho*-functionalized complexes did not give rise to polymerization, the *meta*-functionalized complexes produced mixtures of polymers that comprise amorphous, moderately isotactic, and highly isotactic portions, whose weight ratios were dependent on the reaction temperature. Among the *meta*-functionalized zirconocenes, the di-OMe-substituted ***m*ZrO2** afforded the largest amount of the isotactic portion (82 wt% of the crude polymer), with an [*mmmm*] methyl pentad value of around 90% at 25°C. In contrast, the observation of nearly amorphous polypropylene by the half-functionalized unbridged zirconocene **ASZr** is supportive of the proposition that the generation in situ of rigid *rac*-like ion pairs of the type [*rac*-$L_2ZrP]^+$[Me-MAO]$^-$ through Lewis acid–base interactions between the functional groups and [Me-MAO]$^-$ is responsible for isospecific propylene polymerization with the given class of functionalized unbridged zirconocenes. These results further indicate that the formation of such ion pairs can be favored by difunctionalization at the *meta* position of the phenyl ring with OMe groups.

Experimental Section

General Considerations

All operations were performed under nitrogen gas by using standard Schlenk and glovebox techniques. Anhydrous toluene, CH_2Cl_2, THF, Et_2O, *n*-heptane, and *n*-hexane (Aldrich) were purified by passing through an activated alumina column. All solvents were stored over activated molecular sieves (5 Å, Yakuri Pure Chemicals Co.). Chemicals were used without further purification after purchase from Aldrich (2-bromo-*N,N*-dimethylaniline, 3-bromo-*N,N*-dimethylaniline, 2-methoxyphenylmagnesium bromide, 3-methoxyphenylmagnesium bromide (1.0 M solution in THF), 1-bromo-3,5-dimethoxybenzene, *n*BuLi (2.5 M solution in *n*-hexane), *p*-TsOH, Me_3SiCl) and Strem ($ZrCl_4$, [$ZrCl_4(thf)_2$]). 3,4-Dimethylcyclopent-2-enone,[44] 1-Br-3,5-$(H_2N)_2C_6H_3$,[45] 1-(*p*-$Me_2NC_6H_4$)-3,4-$Me_2C_5H_3$,[34] and 1-(*p*-$CH_3C_6H_4$)-3,4-$Me_2C_5H_3$[37] were prepared according to the literature procedures. $CDCl_3$ was dried over activated molecular sieves (5 Å) and used after vacuum transfer to a Schlenk tube equipped with a J. Young valve. MAO was used as a solid obtained by evaporation of the solvent from a solution of PMAO (pure methylaluminoxane; Chemtura, 30T) in toluene. Polymerization-grade propylene monomer from Honam Petrochemical Corporation was used after purification by passing through Labclear and Oxiclear filters. ^1H and ^{13}C NMR spectra of compounds were recorded on a Bruker Avance 400 spectrometer at ambient temperature. All chemical shifts (δ) are reported in ppm with reference to the residual peaks of $CDCl_3$ for proton ($\delta = 7.24$ ppm) and carbon ($\delta = 77.0$ ppm). Elemental analysis and HR EI-MS were performed on an EA 1110-FISONS instrument (CE Instruments) and a VG Auto Spec spectrometer, respectively, at KAIST.

Syntheses

1-(*o*-$Me_2NC_6H_4$)-3,4-$Me_2C_5H_3$ (***o*N1**): *n*BuLi (1 equiv, 8.0 mL) was added to a solution of 2-bromo-*N,N*-dimethylaniline (4.00 g, 20 mmol) in Et_2O (50 mL) at 0°C. After the mixture was stirred for 2 h at room temperature, it was cooled to −78°C, and then a solution of 3,4-dimethylcyclopent-2-enone (1 equiv, 2.20 g, 20 mmol) in THF (20 mL) was slowly added by cannula. The reaction mixture was allowed to warm slowly to room temperature and stirred overnight. The resulting brownish solution was treated with water (10 mL) followed by concentrated HCl (20 mL). Next, the aqueous layer was isolated and washed with Et_2O (50 mL). The separated aqueous portion was neutralized by treatment with 10% aqueous NaOH. The solution was extracted with Et_2O (2×50 mL), and the combined organic portions were dried over $MgSO_4$. Filtration followed by evaporation of solvent afforded an oily residue. Purification by column chromatography (silica gel, EtOAc/*n*-hexane = 1:10) gave ***o*N1** (1.38 g, 32%) as a pale-yellow oil. ^1H NMR (400.13 MHz, $CDCl_3$): $\delta =$ 7.27 (d, $J = 7.6$ Hz, 1H), 7.12 (t, $J = 7.3$ Hz, 1H), 7.01 (d, $J = 8.0$ Hz, 1H), 6.93 (t, $J = 7.4$ Hz, 1H), 6.71 (s, 1H), 3.36 (s, 2H), 2.65 (s, 6H), 1.96 (s, 3H), 1.89 ppm (s, 3H); $^{13}C\{^1H\}$ NMR (100.62 MHz, $CDCl_3$): $\delta = 151.3$, 142.3, 135.5, 135.2, 134.5, 131.0, 129.2, 126.8, 122.1, 118.4, 46.7, 43.8, 13.3, 12.6 ppm; HRMS (EI): *m*/*z* calcd for $C_{15}H_{19}N$: 213.1518; found: 213.1505.

1-(*m*-$Me_2NC_6H_4$)-3,4-$Me_2C_5H_3$ (***m*N1**): A procedure analogous to that for ***o*N1** was employed with 3-bromo-*N,N*-dimethylaniline (4.00 g, 20 mmol) to afford ***m*N1** (1.27 g, 30%) as a light-yellow solid. ^1H NMR (400.13 MHz, $CDCl_3$): $\delta = 7.17$ (t, $J = 8.0$ Hz, 1H), 6.86–6.83 (m, 2H), 6.64 (s, 1H), 6.59 (d, $J = 9.4$ Hz, 1H), 3.28 (s, 2H), 2.96 (s, 6H), 1.98 (s, 3H), 1.90 ppm (s, 3H); $^{13}C\{^1H\}$ NMR (100.62 MHz, $CDCl_3$): $\delta = 150.9$, 143.3, 137.1, 135.5, 135.4, 131.4, 129.1, 113.7, 111.0, 108.9, 45.4, 40.7, 13.4, 12.6 ppm; HRMS (EI): *m*/*z* calcd for $C_{15}H_{19}N$: 213.1518; found: 213.1514.

1-Br-3,5-$(Me_2N)_2C_6H_3$: A modified literature procedure was employed.[36] *p*-Formaldehyde (1.80 g, 60 mmol) was added to a stirred solution of 5-bromo-*m*-phenylenediamine (2.80 g, 15 mmol) in acetonitrile (30 ml) at 0°C. The reaction mixture was allowed to warm slowly to room temperature and stirred for 3 min. Four portions of sodium cyanoborohydride (3.00 g total, 48 mmol) was added to the reaction mixture over 40 min,

and the mixture was stirred for a further 25 min. Glacial acetic acid was added dropwise until the solution became neutral. Stirring was continued for 45 min with the occasional addition of acetic acid to keep the pH neutral. The solvent was evaporated, and 2 N aqueous KOH was added until the solution was of pH ≈ 9. This solution was extracted with EtOAc (3 × 50 mL), and the combined organic portions were dried over $MgSO_4$, filtered, and evaporated to dryness, which afforded an oily residue. Purification by column chromatography (silica gel, EtOAc/*n*-hexane = 1:9) gave 1-Br-3,5-$(Me_2N)_2C_6H_3$ (0.40 g, 11 %) as an ivory solid. ^{1}H NMR (400.13 MHz, $CDCl_3$): $\delta = 6.26$ (d, $J = 2.1$ Hz, 2H), 5.88 (s, 1H), 2.90 ppm (s, 12H); ^{13}C{^{1}H} NMR (100.62 MHz,$CDCl_3$): $\delta = 152.3$, 124.0, 104.9, 95.4, 40.6 ppm; HRMS (EI): *m*/*z* calcd for $C_{10}H_{15}N_2Br$: 242.0419; found: 242.0415.

1-{3,5-$(Me_2N)_2C_6H_3$}-3,4-$Me_2C_5H_3$ (***m*N2**): A procedure analogous to that for ***o*N1** was employed with 1-bromo-3,5-(*N*,*N*,*N*′,*N*′-tetramethyldiamino)-benzene (1.21 g, 5 mmol) to afford ***m*N2** (0.53 g, 41 %) as a light-yellow solid. ^{1}H NMR (400.13 MHz, $CDCl_3$): $\delta = 6.62$ (s, 1H), 6.33 (d, $J = 2.0$ Hz, 2H), 6.01 (s, 1H), 3.28 (s, 2H), 2.95 (d, 12H), 1.97 (s, 3H), 1.90 ppm (s, 3H); ^{13}C{^{1}H} NMR (100.62 MHz, $CDCl_3$): $\delta = 151.8$, 144.1, 137.5, 135.2, 131.1, 99.9, 96.9, 45.6, 41.0, 13.4, 12.6 ppm; HRMS (EI): *m*/*z* calcd for $C_{17}H_{24}N_2$: 256.1940; found: 256.1952.

1-(*o*-$MeOC_6H_4$)-3,4-$Me_2C_5H_3$ (***o*O1**): A solution of 3,4-dimethylcyclopent-2-enone (2.20 g, 20 mmol) in THF (20 mL) was added slowly to a solution of 2-methoxyphenylmagnesium bromide (1.0 M in THF) in THF (20 mL) by cannula at −78 °C. The reaction mixture was allowed to warm slowly to room temperature and stirred overnight. The resulting orange solution was treated with saturated aqueous NH_4Cl (50 mL) to stop the reaction. Next, the organic portion was separated, and the aqueous layer was further extracted with Et_2O (50 mL). The combined organic portions were dried over $MgSO_4$, filtered, and evaporated to dryness to afford a light-orange oily product. The crude product was redissolved in CH_2Cl_2 (30 mL), and then a catalytic amount of *p*-TsOH (≈0.1 g) was added as solid to the solution at room temperature, followed by stirring for about 60 min. Evaporation of the solvent and purification by column chromatography (silica gel, EtOAc/hexane = 1:10) afforded ***o*O1** (1.20 g, 30 %) as an ivory solid. ^{1}H NMR (400.13 MHz, $CDCl_3$): $\delta = 7.38$ (d, $J =$ 7.5 Hz, 1H), 7.12 (t, $J = 7.7$ Hz, 1H), 6.92–6.87 (m, 3H), 3.88 (s, 3H), 3.35 (s, 2H), 1.97 (s, 3H), 1.90 ppm (s, 3H); ^{13}C{^{1}H} NMR (100.62 MHz, $CDCl_3$): $\delta = 156.7$, 139.0, 135.8, 135.6, 135.5, 127.6, 126.7, 125.6, 120.5, 111.0, 55.2, 47.4, 13.3, 12.6 ppm; HRMS (EI): *m*/*z* calcd for $C_{14}H_{16}O$: 200.1201; found: 200.1223.

1-(*m*-$MeOC_6H_4$)-3,4-$Me_2C_5H_3$ (***m*O1**): A procedure analogous to that for ***o*O1** was employed with 3-methoxyphenylmagnesium bromide (1.0 M in THF, 20 mL), which afforded ***m*O1** (1.00 g, 25 %) as a pale-yellow oil. ^{1}H NMR (400.13 MHz, $CDCl_3$): $\delta = 7.18$ (t, $J = 7.9$ Hz, 1H), 7.03 (d, $J =$ 7.7 Hz, 1H), 6.96 (t, $J = 1.7$ Hz, 1H), 6.69 (dd, $J = 8.1$, 2.5 Hz, 1H), 6.64 (s, 1H), 3.80 (s, 3H), 3.24 (s, 2H), 1.96 (s, 3H), 1.88 ppm (s, 3H); ^{13}C{^{1}H} NMR (100.62 MHz, $CDCl_3$): $\delta = 159.8$, 142.3, 137.8, 136.1, 135.5, 132.1, 129.4, 117.3, 111.4, 110.2, 55.2, 45.3, 13.4, 12.6 ppm; HRMS (EI): *m*/*z* calcd for $C_{14}H_{16}O$: 200.1201; found: 200.1208.

1-{3,5-$(MeO)_2C_6H_3$}-3,4-$Me_2C_5H_3$ (***m*O2**): A solution of 1-bromo-3,5-dimethoxybenzene (4.34 g, 20 mmol) in Et_2O (20 mL) was treated with *n*BuLi (1 equiv, 8.0 mL) at 0 °C. After the mixture was stirred for 2 h at room temperature, a solution of 3,4-dimethylcyclopent-2-enone (1 equiv, 2.20 g, 20 mmol) in THF (20 mL) was slowly added by cannula at −78 °C. The reaction mixture was allowed to warm slowly to room temperature and stirred overnight. Further workup and dehydration were carried out in a manner analogous to the procedure for ***o*O1**. Recrystallization from ethanol at −20 °C afforded ***m*O2** (1.32 g, 33 %). ^{1}H NMR (400.13 MHz, $CDCl_3$): $\delta = 6.64$ (s, 1H), 6.59 (d, $J = 2.2$ Hz, 2H), 6.28 (t, $J = 2.1$ Hz, 1H), 3.79 (s, 6H), 3.23 (s, 2H), 1.96 (s, 3H), 1.88 ppm (s, 3H); ^{13}C{^{1}H} NMR (100.62 MHz, $CDCl_3$): $\delta = 160.9$, 142.3, 138.3, 136.2, 135.4, 132.4, 102.8, 98.3, 55.3, 45.4, 13.4, 12.6 ppm; HRMS (EI): *m*/*z* calcd for $C_{15}H_{18}O_2$: 230.1307; found: 230.1297.

[{1-(*o*-$Me_2NC_6H_4$)-3,4-$Me_2C_5H_2$}$_2$$ZrCl_2$] (***o*ZrN1**): A solution of ***o*N1** (0.853 g, 4.0 mmol) in Et_2O (20 mL) was treated with *n*BuLi (1 equiv, 1.6 mL) at −78 °C. The reaction mixture was allowed to warm to room temperature and stirred for 4 h. The resulting reaction mixture was evaporated to dryness, and the lithium salt of ***o*N1** was combined with [$ZrCl_4$(thf)$_2$] (0.5 equiv, 0.755 g, 2 mmol). Toluene (30 mL) was then introduced into the solid mixture at −78 °C. After the reaction mixture was allowed to warm to room temperature, it was stirred at 60 °C overnight. The yellow reaction mixture was filtered through a celite pad, and the filtrate was evaporated to dryness. Washing with *n*-hexane followed by drying in vacuo afforded ***o*ZrN1** (0.616 g, 52 %). Single crystals suitable for X-ray diffraction were grown from CH_2Cl_2/*n*-hexane at −20 °C. ^{1}H NMR (400.13 MHz, $CDCl_3$): $\delta = 7.45$ (d, $J = 7.8$ Hz, 2H), 7.18–7.02 (m, 4H), 7.00 (t, $J = 7.3$ Hz, 2H), 6.68 (s, 4H), 2.62 (s, 12H), 1.71 ppm (s, 12H); ^{13}C{^{1}H} NMR (100.62 MHz, $CDCl_3$): $\delta = 151.4$, 130.0, 127.8, 127.6, 126.6, 122.9, 121.7, 119.0, 118.6, 44.5, 13.2 ppm; elemental analysis: calcd for $C_{30}H_{36}Cl_2N_2Zr$: C 61.41, H 6.18, N 4.77; found: C 60.46, H 6.23, N 4.70.

[{1-(*m*-$Me_2NC_6H_4$)-3,4-$Me_2C_5H_2$}$_2$$ZrCl_2$] (***m*ZrN1**): A procedure analogous to that for ***o*ZrN1** with an ***m*N1** ligand was employed, which resulted in bright-yellow crystals of ***m*ZrN1** (0.567 g, 48 %). Single crystals were grown from Et_2O/*n*-hexane at −20 °C. ^{1}H NMR (400.13 MHz, $CDCl_3$): $\delta = 7.29$ (t, $J = 8.0$ Hz, 2H), 6.81 (d, $J = 7.7$ Hz, 2H), 6.77 (s, 2H), 6.66 (d, $J = 8.3$ Hz, 2H), 6.21 (s, 4H), 3.00 (s, 12H), 1.82 ppm (s, 12H); ^{13}C{^{1}H} NMR (100.62 MHz, $CDCl_3$): $\delta = 151.1$, 134.3, 129.7, 128.0, 123.5, 116.6, 113.5, 111.6, 109.6, 40.6, 13.3 ppm; elemental analysis: calcd for $C_{30}H_{36}Cl_2N_2Zr$: C 61.41, H 6.18, N 4.77; found: C 62.04, H 6.37, N 4.77.

[{1-(3,5-$(Me_2N)_2C_6H_3$)-3,4-$Me_2C_5H_2$}$_2$$ZrCl_2$] (***m*ZrN2**): By following the above procedure for ***o*ZrN1** with ***m*N2** (0.513 g, 2.0 mmol), ***m*ZrN2** (0.321 g, 48 %) was obtained as a light-yellow solid. ^{1}H NMR (400.13 MHz, $CDCl_3$): $\delta = 6.26$ (s, 4H), 6.25 (d, $J = 2.2$ Hz, 4H), 6.00 (s, 2H), 2.98 (s, 24H), 1.85 ppm (s, 12H); ^{13}C{^{1}H} NMR (100.62 MHz, $CDCl_3$): δ 152.1, 134.8, 127.7, 124.5, 116.9, 100.0, 96.6, 40.8, 13.4 ppm; elemental analysis: calcd for $C_{34}H_{46}Cl_2N_4Zr$: C 60.69, H 6.89, N 8.33; found: C 60.45, H 6.80, N 8.66.

[{1-(*o*-$MeOC_6H_4$)-3,4-$Me_2C_5H_2$}$_2$$ZrCl_2$] (***o*ZrO1**): By following the above procedure for ***o*ZrN1** with ***o*O1** (0.801 g, 4.0 mmol), ***o*ZrO1** (0.504 g, 45 %) was obtained as yellow crystals. Single crystals were grown from CH_2Cl_2/*n*-hexane at −20 °C. ^{1}H NMR (400.13 MHz, $CDCl_3$): $\delta = 7.36$ (dd, $J = 7.9$, 1.7 Hz, 2H), 7.26 (d, $J = 8.9$ Hz, 2H), 7.01–6.97 (m, 4H), 6.40 (s, 4H), 3.91 (s, 6H), 1.83 ppm (s, 12H); ^{13}C{^{1}H} NMR (100.62 MHz, $CDCl_3$): $\delta = 155.7$, 128.4, 128.3, 127.8, 122.4, 120.8, 119.8, 118.1, 111.3, 55.1, 13.2 ppm; elemental analysis: calcd for $C_{28}H_{30}Cl_2O_2Zr$: C 59.98, H 5.39; found: C 59.97, H 5.64.

[{1-(*m*-$MeOC_6H_4$)-3,4-$Me_2C_5H_2$}$_2$$ZrCl_2$] (***m*ZrO1**): A procedure analogous to that for ***o*ZrN1** was employed with ***m*O1** (0.801 g, 4.0 mmol), which resulted in ***m*ZrO1** (0.519 g, 46 %) as a light-yellow solid after washing with Et_2O (10 mL) and *n*-hexane (10 mL) followed by drying under vacuum. ^{1}H NMR (400.13 MHz, $CDCl_3$): $\delta = 7.35$ (t, $J = 8.0$ Hz, 2H), 7.05 (d, $J =$ 8.1 Hz, 2H), 6.98 (t, $J = 2.3$ Hz, 2H), 6.82 (dd, $J = 8.2$, 2.6 Hz, 2H), 6.22 (s, 4H), 3.85 (s, 6H), 1.79 ppm (s, 12H); ^{13}C{^{1}H} NMR (100.62 MHz, $CDCl_3$): $\delta = 160.2$, 134.8, 130.2, 128.3, 122.1, 117.6, 116.4, 113.0, 110.8, 55.3, 13.2 ppm; elemental analysis: calcd for $C_{28}H_{30}Cl_2O_2Zr$: C 59.98, H 5.39; found: C 60.59, H 5.62.

[{1-(2,4-$(MeO)_2C_6H_3$)-3,4-$Me_2C_5H_2$}$_2$$ZrCl_2$] (***m*ZrO2**): A procedure analogous to that for ***o*ZrN1** was employed with ***m*O2** (0.921 g, 4.0 mmol), which afforded ***m*ZrO2** (0.447 g, 36 %) as a yellow solid. Single crystals suitable for X-ray structural determination were obtained by cooling a solution of ***m*ZrO2** in Et_2O/*n*-hexane at −20 °C. ^{1}H NMR (400.13 MHz, $CDCl_3$): $\delta = 6.59$ (d, $J = 2.2$ Hz, 4H), 6.39 (t, $J = 2.1$ Hz, 2H), 6.19 (s, 4H), 3.83 (s, 12H), 1.85 ppm (s, 12H); ^{13}C{^{1}H} NMR (100.62 MHz, $CDCl_3$): $\delta = 161.4$, 135.5, 128.3, 122.3, 116.7, 103.5, 99.4, 55.4, 13.3 ppm; elemental analysis: calcd for $C_{30}H_{34}Cl_2O_4Zr$: C 58.05, H 5.52; found: C 58.61, H 5.66.

[{1-(*p*-$Me_2NC_6H_4$)-3,4-$Me_2C_5H_2$}{1-(*p*-tolyl)-3,4-$Me_2C_5H_2$}$ZrCl_2$] (**ASZr**): A solution of 1-(*p*-tolyl)-3,4-$Me_2C_5H_3$ (0.369 g, 2.0 mmol) in Et_2O (20 mL) was treated with *n*BuLi (1 equiv, 0.8 mL) at −78 °C. The reaction mixture was allowed to warm to room temperature and stirred for 4 h. The resulting lithium salt was subsequently treated with excess Me_3SiCl (3.0 equiv, 0.76 mL) in THF at 0 °C. After the reaction mixture was warmed to room temperature, it was further stirred overnight. The resulting reaction mixture was evaporated to dryness and extracted with *n*-

hexane (30 mL). Drying in vacuo afforded 1-(*p*-tolyl)-3,4-$Me_2C_5H_2SiMe_3$ (0.51 g, 99%) as an ivory solid. ^{1}H NMR (400.13 MHz, $CDCl_3$): δ = 7.19 (d, J = 8.0 Hz, 2H), 7.05 (d, J = 8.1 Hz, 2H), 6.51 (s, 1H), 3.65 (s, 1H), 2.30 (s, 3H), 2.00 (s, 3H), 1.91 (s, 3H), −0.23 ppm (t, 9H); ^{13}C{^{1}H} NMR (100.62 MHz, $CDCl_3$): δ = 144.6, 137.1, 135.4, 135.0, 134.7, 129.8, 128.8, 126.3, 53.5, 21.1, 14.6, 12.5, −2.0 ppm. Next, a slurry of $ZrCl_4$ (0.420 g, 1.80 mmol) in *n*-heptane was added to a solution of 1-(*p*-tolyl)-3,4-$Me_2C_5H_2SiMe_3$ (0.50 g, 1.94 mmol) in *n*-heptane (10 mL) by cannula at −78 °C. After the reaction mixture was warmed to room temperature, it was stirred overnight. Washing with *n*-hexane (2×10 mL) followed by drying in vacuo afforded [{1-(*p*-tolyl)-3,4-$Me_2C_5H_2$}$ZrCl_3$] (0.57 g, 83%) as a yellow-brown solid. ^{1}H NMR (400.13 MHz, $CDCl_3$): δ 7.49 (d, J = 8.1 Hz, 2H), 7.20 (d, J = 7.9 Hz, 2H), 6.76 (s, 2H), 2.36 (s, 3H), 2.34 (s, 6H). The obtained solid was combined with the lithium salt of 1-(*p*-$Me_2NC_6H_4$)-3,4-$Me_2C_5H_3$ (0.32 g, 1.5 mmol) in a dry box. Toluene (20 mL) was then introduced to the solid mixture at −78 °C. After the reaction mixture was allowed to warm to room temperature, it was heated to 60 °C and stirred at this temperature overnight. The reaction mixture was filtered through a celite pad, and the filtrate was evaporated to dryness. Washing with *n*-hexane followed by drying in vacuo afforded **ASZr** (0.616 g, 52%). Single crystals were grown from CH_2Cl_2/*n*-hexane at −20 °C. ^{1}H NMR (400.13 MHz, $CDCl_3$): δ = 7.37–7.32 (m, 4H), 7.23 (d, J = 7.6 Hz, 2H), 6.77 (d, J = 8.8 Hz, 2H), 6.21 (s, 2H), 6.13 (s, 2H), 3.00 (s, 6H), 2.38 (s, 3H), 1.79 (s, 6H), 1.75 ppm (s, 6H); ^{13}C{^{1}H} NMR (100.62 MHz, $CDCl_3$): δ = 149.8, 137.0, 130.7, 129.7, 127.8, 127.3, 126.3, 125.1, 124.2, 122.5, 121.6, 115.8, 114.7, 112.6, 40.5, 21.2, 13.2, 13.1 ppm; elemental analysis: calcd for $C_{29}H_{33}Cl_2NZr$: C 62.45, H 5.96, N 2.51; found: C 62.06, H 6.05, N 2.77.

X-ray Structure Determination

Crystallographic measurement was performed by using a Bruker Apex II-CCD area detector diffractometer with graphite-monochromated $Mo_{K\alpha}$ radiation (λ = 0.71073 Å). A specimen of suitable size and quality was selected and mounted onto a glass capillary. Structures were solved by direct methods, and all non-hydrogen atoms were subjected to anisotropic refinement by full-matrix least squares on F^2 with the SHELXTL/PC package. Hydrogen atoms were placed at their geometrically calculated positions and refined as riding on the corresponding carbon atoms with isotropic thermal parameters. Detailed crystallographic data for ***o*ZrN1**, ***m*ZrN1**, ***o*ZrO1,** ***m*ZrO2**, and **ASZr** are given in Table 1. CCDC-689731 (***o*ZrN1**), -689732 (***m*ZrN1**), -689733 (***o*ZrO1**), -689734 (***m*ZrO2**), and -689735 (**ASZr**) contain the supplementary crystallographic data for this paper. These data can be obtained free of charge from the Cambridge Crystallographic Data Centre at www.ccdc.cam.ac.uk/data_request/cif.

Propylene Polymerization

Freshly distilled toluene (48 mL) was transferred into a well-degassed 250-mL glass reactor charged with preweighed s-MAO (solid MAO; [Al]/[Zr] = 1000), and the temperature was adjusted by using an external bath. After saturation of propylene monomer at 1 bar with vigorous stirring for 30 min, polymerization was started by the injection of a solution of catalyst (5.0 μmol of Zr) in toluene (2.0 mL). All the polymerization reactions were quenched by the injection of acidified ethanol (10% HCl in EtOH; 5 mL) after the desired reaction time (t_p). The resulting polypropylenes were further precipitated by addition of acidified EtOH (200 mL). After the mixture was stirred for 1–2 h, the polypropylenes were collected by filtration or decantation of the solution (in the case of a sticky polymer) and washed with EtOH several times. The resulting polypropylenes were dried in a vacuum oven at 80 °C to constant weight.

Ethylene Polymerization

Ethylene polymerization with ***m*ZrN2** was performed analogously at 1 bar ethylene pressure under MAO activation ([Al]/[Zr] = 1000).

Polymer Extraction

Solvent extraction of all the polypropylenes was carried out by using a Soxhlet extractor. A preweighed sample of polypropylene was first extracted with boiling Et_2O (100 mL) for 12 h. The residue was then extracted with boiling *n*-heptane (100 mL) for another 12 h. Evaporation of the resulting solutions by a rotary evaporator afforded diethyl ether soluble and diethyl ether insoluble/*n*-heptane-soluble portions of polypropylene, respectively. The obtained portions and the remaining residue (diethyl ether insoluble/*n*-heptane-insoluble portion) were finally dried under vacuum at 80 °C to constant weight.

Polymer Analysis

^{13}C NMR spectra of the polypropylenes were recorded on a Bruker Avance 400 (^{13}C: 100.62 MHz) spectrometer for the diethyl ether soluble and diethyl ether insoluble/*n*-heptane-soluble portions at 100 °C and on a Bruker AMAX 500 (^{13}C: 125.77 MHz) spectrometer for the *n*-heptane-insoluble portions at 120 °C with a pulse angle of 90°, an acquisition time of 2 s, and a relaxation delay of 8 s. The samples were dissolved in 1,1,2,2,-[D_2]tetrachloroethane to form a 10 wt% solution (≈90 mg/0.5 mL) in 5-mm tubes. All the measurements were performed after complete dissolution by warming (for the diethyl ether soluble and diethyl ether insoluble/*n*-heptane-soluble portions) or preheating (for the *n*-heptane-insoluble portions) to about 110 °C in an oil bath. The chemical shift of the residual peak of the solvent (δ = 74.1 ppm) was used as an internal standard. Peak assignments and the determination of methyl pentad sequence distributions were made according to the reported literature.[12] The molecular weights (M_w) and MWDs (M_w/M_n) of the polypropylenes were determined by GPC (Polymer Laboratories PL-GPC 220, 140 °C) in 1,2,4-trichlorobenzene with standard polystyrenes as a reference. The melting temperatures (T_m) of the polypropylenes were measured by DSC (TA Instruments 2910 MDSC) at a heating rate of 10 °C min^{-1}. Any thermal history in the polymers was eliminated by first heating the samples to 180 °C at 20 °C min^{-1}, cooling to 30 °C at 20 °C min^{-1}, and then recording the second DSC scan from 30 to 180 °C.

Acknowledgements

Financial support from the Korea Science and Engineering Foundation, the BK 21 Project, the PAL 2008-2041-05 and the POMRC 10016538 are gratefully acknowledged. We thank Honam Petrochemical Corp. for the GPC and DSC analyses.

[1] H. Braunschweig, F. M. Breitling, *Coord. Chem. Rev.* **2006**, *250*, 2691–2720.
[2] P. Corradini, G. Guerra, L. Cavallo, *Acc. Chem. Res.* **2004**, *37*, 231–241.
[3] V. C. Gibson, S. K. Spitzmesser, *Chem. Rev.* **2003**, *103*, 283–316.
[4] G. W. Coates, P. D. Hustad, S. Reinartz, *Angew. Chem.* **2002**, *114*, 2340–2361; *Angew. Chem. Int. Ed.* **2002**, *41*, 2236–2257.
[5] J. Schellenberg, N. Tomotsu, *Prog. Polym. Sci.* **2002**, *27*, 1925–1982.
[6] J. A. Gladysz, *Chem. Rev.* **2000**, *100*, 1167–1682.
[7] G. J. P. Britovsek, V. C. Gibson, D. F. Wass, *Angew. Chem.* **1999**, *111*, 448–468; *Angew. Chem. Int. Ed.* **1999**, *38*, 428–447.
[8] A. L. McKnight, R. M. Waymouth, *Chem. Rev.* **1998**, *98*, 2587–2598.
[9] H. H. Brintzinger, D. Fischer, R. Mülhaupt, B. Rieger, R. M. Waymouth, *Angew. Chem.* **1995**, *107*, 1255–1283; *Angew. Chem. Int. Ed. Engl.* **1995**, *34*, 1143–1170.
[10] J. A. Ewen, *Macromol. Symp.* **1995**, *89*, 181–196.
[11] *Stereoselective Polymerization with Single-Site Catalysts* (Eds.: L. S. Baugh, J. A. M. Canich), CRC, Boca Raton, **2008**, pp. 1–342.
[12] L. Resconi, L. Cavallo, A. Fait, F. Piemontesi, *Chem. Rev.* **2000**, *100*, 1253–1346.
[13] G. W. Coates, *Chem. Rev.* **2000**, *100*, 1223–1252.
[14] J. A. Ewen, R. L. Jones, A. Razavi, J. D. Ferrara, *J. Am. Chem. Soc.* **1988**, *110*, 6255–6256.
[15] W. Kaminsky, K. Külper, H. H. Brintzinger, F. R. W. P. Wild, *Angew. Chem.* **1985**, *97*, 507–508; *Angew. Chem. Int. Ed. Engl.* **1985**, *24*, 507–508.
[16] J. A. Ewen, *J. Am. Chem. Soc.* **1984**, *106*, 6355–6364.

[17] M. Knickmeier, G. Erker, T. Fox, *J. Am. Chem. Soc.* **1996**, *118*, 9623–9630.
[18] G. Erker, M. Aulbach, M. Knickmeier, D. Wingbermuehle, C. Krueger, M. Nolte, S. Werner, *J. Am. Chem. Soc.* **1993**, *115*, 4590–4601.
[19] G. Erker, B. Temme, *J. Am. Chem. Soc.* **1992**, *114*, 4004–4006.
[20] G. Erker, R. Nolte, R. Aul, S. Wilker, C. Krüger, R. Noe, *J. Am. Chem. Soc.* **1991**, *113*, 7594–7602.
[21] A. L. Lincoln, G. M. Wilmes, R. M. Waymouth, *Organometallics* **2005**, *24*, 5828–5835.
[22] S. Lin, R. M. Waymouth, *Acc. Chem. Res.* **2002**, *35*, 765–773.
[23] G. M. Wilmes, J. L. Polse, R. M. Waymouth, *Macromolecules* **2002**, *35*, 6766–6772.
[24] G. M. Wilmes, S. Lin, R. M. Waymouth, *Macromolecules* **2002**, *35*, 5382–5387.
[25] S. Lin, C. D. Tagge, R. M. Waymouth, M. Nele, S. Collins, J. C. Pinto, *J. Am. Chem. Soc.* **2000**, *122*, 11275–11285.
[26] J. L. Maciejewski Petoff, C. L. Myers, R. M. Waymouth, *Macromolecules* **1999**, *32*, 7984–7989.
[27] Y. Hu, M. T. Krejchi, C. D. Shah, C. L. Myers, R. M. Waymouth, *Macromolecules* **1998**, *31*, 6908–6916.
[28] J. L. Maciejewski Petoff, M. D. Bruce, R. M. Waymouth, A. Masood, T. K. Lal, R. W. Quan, S. J. Behrend, *Organometallics* **1997**, *16*, 5909–5916.
[29] E. Hauptman, R. M. Waymouth, J. W. Ziller, *J. Am. Chem. Soc.* **1995**, *117*, 11586–11587.
[30] G. W. Coates, R. M. Waymouth, *Science* **1995**, *267*, 217–219.
[31] V. Busico, V. Van Axel Castelli, P. Aprea, R. Cipullo, A. Segre, G. Talarico, M. Vacatello, *J. Am. Chem. Soc.* **2003**, *125*, 5451–5460.
[32] V. Busico, R. Cipullo, W. P. Kretschmer, G. Talarico, M. Vacatello, V. Van Axel Castelli, *Angew. Chem.* **2002**, *114*, 523–526; *Angew. Chem. Int. Ed.* **2002**, *41*, 505–508.
[33] A. Razavi, J. L. Atwood, *J. Am. Chem. Soc.* **1993**, *115*, 7529–7530.
[34] S. K. Kim, H. K. Kim, M. H. Lee, S. W. Yoon, Y. Do, *Angew. Chem.* **2006**, *118*, 6309–6312; *Angew. Chem. Int. Ed.* **2006**, *45*, 6163–6166.
[35] S. K. Kim, H. K. Kim, M. H. Lee, S. W. Yoon, Y. Do, *Chem. Eur. J.* **2007**, *13*, 9107–9114.
[36] D. Samanta, S. Sawoo, S. Patra, M. Ray, M. Salmain, A. Sarkar, *J. Organomet. Chem.* **2005**, *690*, 5581–5590.
[37] S. Jüngling, R. Mülhaupt, H. Plenio, *J. Organomet. Chem.* **1993**, *460*, 191–195.
[38] G. H. Llinas, M. Mena, F. Palacios, P. Royo, R. Serrano, *J. Organomet. Chem.* **1988**, *340*, 37–40.
[39] C. D. Tagge, R. L. Kravchenko, T. K. Lal, R. M. Waymouth, *Organometallics* **1999**, *18*, 380–388.
[40] M. H. Lee, Y. Do, *J. Organomet. Chem.* **2005**, *690*, 1240–1248.
[41] K. Kimura, K. Takaishi, T. Matsukawa, T. Yoshimura, H. Yamazaki, *Chem. Lett.* **1998**, *27*, 571–572.
[42] A. Lehtinen, R. Paukkeri, *Macromol. Chem. Phys.* **1994**, *195*, 1539–1556.
[43] V. Busico, R. Cipullo, *Prog. Polym. Sci.* **2001**, *26*, 443–533.
[44] J. M. Conia, M. L. Leriverend, *Bull. Soc. Chim. Fr.* **1970**, 2981–2991.
[45] M.-A. Kakimoto, M. Yoneyama, Y. Imai, *J. Polym. Sci. Part A: Polym. Chem.* **2000**, *38*, 3911–3918.

Received: June 4, 2008
Published online: September 2, 2008

